

Electric Field Assisted Growth of Highly Surface Enhanced Raman Active Gold Nanotriangles

P. R. Sajanlal and T. Pradeep*

DST Unit on Nanoscience (DST UNS), Department of Chemistry and Sophisticated Analytical Instrument Facility, Indian Institute of Technology Madras, Chennai 600036, India

A comparative study of the surface-enhanced Raman scattering (SERS) effect of the spherical gold nanoparticles (NPs) and highly uniform and oriented gold nanotriangles (NTs), anchored on indium tin oxide (ITO) coated conducting glass surfaces is reported. Contact and non-contact mode atomic force microscopic (AFM) analyses confirmed that all the triangles observed are equilateral and uniformly stacked. The NTs-coated ITO exhibited intense near-infrared (NIR) absorption and showed an extremely strong SERS activity than the spherical NPs. The NTs showed a very good SERS enhancement factor on the order of 4×10^8 . The results are interpreted in terms of the increased density of hot spots on the NTs-coated surface.

Keywords: Gold Nanotriangles, ITO, Seed-Mediated Method, Atomic Force Microscopy, SERS.

1. INTRODUCTION

Surface-enhanced Raman scattering has attracted considerable attention due to its unique advantages over other surface characterization techniques.¹ It is a powerful analytical tool for obtaining vibrational information of molecules on metallic substrates. SERS can be exploited for sensitive and selective molecular identification and is being extensively used for biological and chemical sensing.² The SERS phenomenon is often explained by the electromagnetic and chemical enhancement mechanisms.³ The chemical enhancement mechanism involves charge transfer excitation⁴ between the analyte molecules and the metal particles, whereas the electromagnetic mechanism is dominated by plasmon excitation leading to hot spots⁵ around nano-sized metal particles by an increase in the local optical field. The magnitude of electromagnetic enhancement is highly dependent on the plasmon absorption of the substrate. The enhancement of a given electromagnetic field in the proximity of a nanoparticle critically depends on the size, shape and orientation of the nanoparticles. Gold NTs are a promising class of nanomaterials for the SERS study because of strong enhancement of electric fields at the vertices.⁶ In order to fabricate SERS based reliable and reproducible functional materials and devices, it is necessary to have a periodic and ordered assembly of these nanoparticles on solid planar substrates.

Several strategies have been employed for the fabrication of triangular metal nanoparticles onto planar surfaces such as nanosphere lithography,⁷ seed-mediated method,⁸ galvanic displacement reactions,⁹ sputter deposition and thermal vapor deposition.¹⁰ Here we adopted a method reported from our group¹¹ for making highly SERS active and oriented gold NTs array on ITO surfaces. These NTs-coated substrate exhibited high NIR absorption also. In this paper we have provided a comparative study of the SERS activity of the NTs-coated ITO as well as NPs immobilized ITO surfaces. The results show strong SERS activity of NTs over NPs.

2. EXPERIMENTAL DETAILS

Tetrachloroauric acid trihydrate ($\text{HAuCl}_4 \cdot 3\text{H}_2\text{O}$), cetyltrimethylammonium bromide (CTAB), ascorbic acid, sodium citrate and crystal violet (CV) were purchased from CDH, India. Aminopropyltrimethoxysilane (APTMS) and sodium borohydride (NaBH_4) were purchased from Aldrich. Optically transparent ITO with a resistivity of $70 \Omega/\text{cm}$ was used throughout this work. All chemicals were used as such without further purification. Triply distilled water was used throughout the experiments.

The ITO glass slide of dimensions $1 \text{ cm} \times 2 \text{ cm}$ were washed with a mild detergent solution, ethanol and finally with pure water. It was then soaked in 10% HCl solution for activation, washed with water and dried under a

*Author to whom correspondence should be addressed.

stream of nitrogen. These plates were annealed at 400 °C for 8 h and cooled in a desiccator. The glass slides were dipped in 30 mM APTMS solution in methanol for 1 h. Afterwards, they were washed with methanol and water in sequence and kept at 100 °C for 1 h.

Spherical gold nanoparticles were synthesized by NaBH_4 reduction method.¹² The silanized ITO plates were immersed in gold nanoparticles seed solution for 20 min. It is then washed and dried. The seed immobilized substrate and an identical blank ITO glass plate were kept at 5 mm apart such that the conducting surfaces faced each other and were connected to the $-ve$ and $+ve$ terminals of a DC power supply. The distance was maintained using a Teflon[®] spacer. A potential of 110 mV was applied between the plates. The area of contact of both electrodes in the growth solution was fixed at 1 cm^2 . The growth vessel was kept inside an ice bath throughout the process. 20 mL, 100 mM CTAB solution was added and kept for 3 min. After this, 900 μL , 10 mM $\text{HAuCl}_4 \cdot 3\text{H}_2\text{O}$ was added followed by 100 μL , 100 mM ascorbic acid. The set-up was allowed to stand undisturbed for 1 h. After the completion of growth, the substrate was taken out, washed using distilled water and was characterized. The edge length of the as prepared NTs was found to increase by introducing excess amount of Au^{3+} (100 μl , 10 mM) and ascorbic acid (100 μl , 100 mM). Experiments were also carried out after varying the parameters, as described in the text. For the SERS studies, we prepared the crystal violet solution of various concentrations in water.

Atomic force microscopy (AFM) and Raman spectroscopy were conducted using AFM-CRM 200 spectrometer of WiTec GmbH. Scanning electron microscopic (SEM) images were taken in a FEI QUANTA-200 SEM. For the vibrational characterization, the substrate was mounted on the sample stage of a confocal Raman microscope (CRM). The spectra were collected with 514.5 nm Ar ion laser. The beam size used was $<1 \mu\text{m}$. The back-scattered light was collected by a 60 \times objective and sent to the spectrometer through a multimode fibre. Data from liquid droplets were collected with a liquid immersion objective. UV-vis-NIR measurements were done using a Varian 5E spectrometer in the range of 200–2500 nm. XRD data were collected with a Shimadzu XD-D1 diffractometer using $\text{Cu K}\alpha$ radiation ($\lambda = 1.54 \text{ \AA}$). The samples were scanned in the 2θ range of 10–90 degrees.

3. RESULTS AND DISCUSSION

The NTs were synthesized on the ITO plate as described in the experimental section. The characterization of these NTs was done by optical absorption measurements, AFM, SEM, optical microscope and XRD (details are presented in Ref. [11]). Figure 1 shows the UV-vis spectra of the AuNPs (trace A) and NTs-coated ITO (trace B). The NPs-coated substrate exhibited an absorption maximum

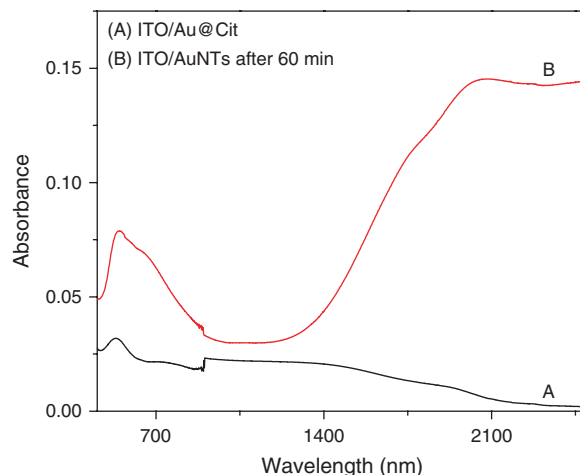


Fig. 1. UV-vis spectra of NPs-coated ITO (trace A) and NTs-coated ITO (trace B) prepared using 10 mM Au^{3+} after 1 h growth.

at 520 nm, which is due to the surface plasmon resonance (SPR) of spherical gold nanoparticles. The broad peak in the NIR region and that at 540 nm of the NTs-coated substrate (trace B) are attributed to in-plane¹³ and out of plane^{6,13} SPRs of NTs. The quadrupole resonance¹³ of the NTs was observed as a broad band at 730–800 nm.

We analyzed the sample in the non-contact mode AFM. Figures 2(A) and (B) are the respective large area topographic and phase contrast mode AFM images of the NTs. The image shows that a large number of NTs are formed on the ITO after 1 h of the reaction by applying a potential of 110 mV. From the height profile analysis (inset of Fig. 2(B)) it is confirmed that the NTs are ~ 375 nm in length and have a thickness of ~ 20 nm. We have done a range of control experiments to understand the various factors important in this process.¹¹ From these observations, we came into a conclusion that the temperature and the applied potential play important roles in the formation of the NTs. We optimized the experimental condition in order to yield oriented equilateral NTs.¹¹ Figure 2(C) shows the contact mode AFM image of the NPs-coated on the ITO surface. The NPs were slightly aggregated on the surface of ITO. The five diffraction peaks of face centered cubic (fcc) gold, (111), (200), (220), (311) and (222) are observed in the XRD (Fig. 2(D)) of the NTs-coated ITO. The intensity ratio of the (111) to (200) peak in the XRD pattern of nanoplates was higher than the bulk value. This result suggests that the Au nanoplates are rich in (111) planes and are lying flat on the surface, as seen in AFM. Peaks other than (111) are seen as the X-ray looks at a larger region where other nanostructures could also be present.

The SEM image of the NTs formed on the ITO surface after 1 h growth is shown in Figure 3(A). The SEM images taken from various areas of the ITO show the presence of NTs, which are stacked one over the other. Because of the large edge length to thickness ratio, the

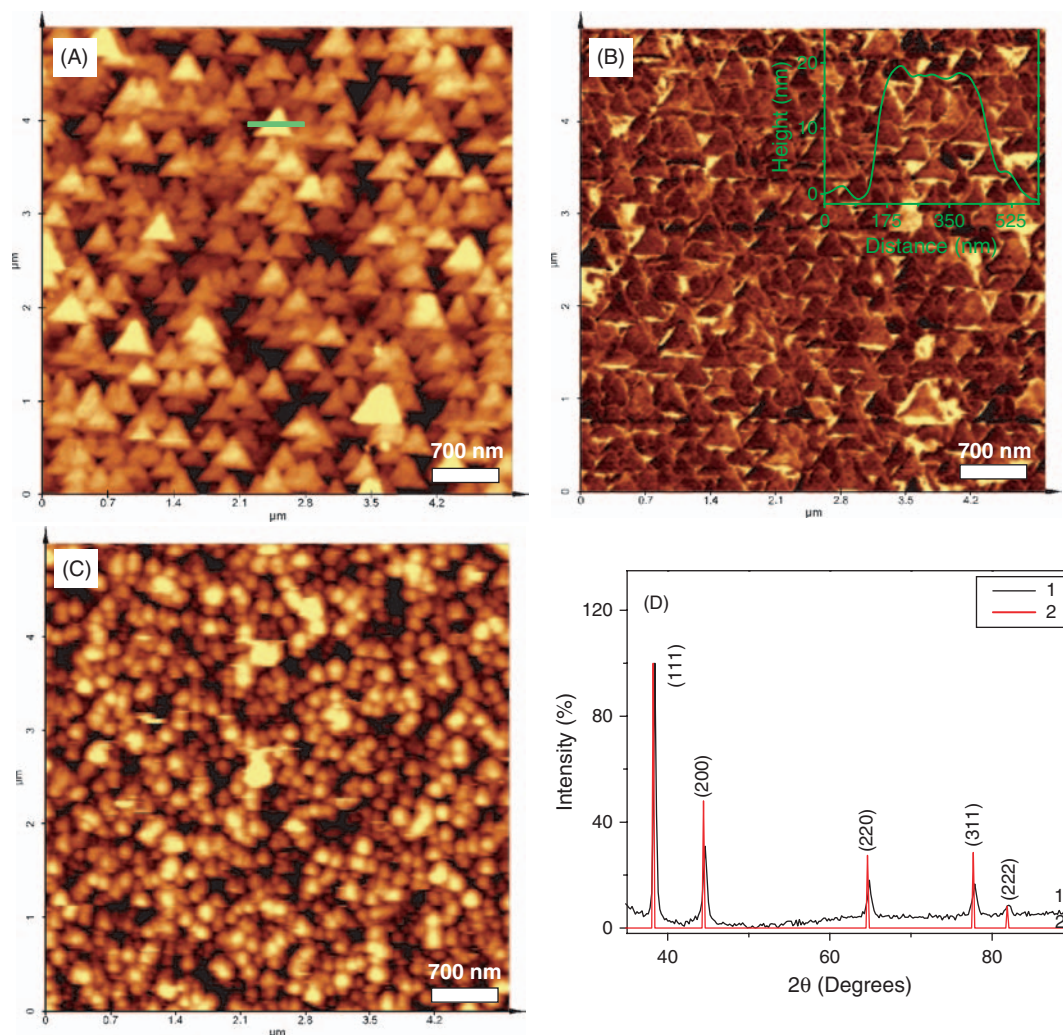


Fig. 2. The large area non-contact mode topographic (A) and phase (B) AFM images of NTs formed on ITO after 1 h. The height profile of one NT along the dashed line in A is shown in the inset of B. (C) Contact mode AFM image of the NPs-coated ITO and (D) X-ray diffraction pattern of NTs formed on ITO after 1 h growth (1). The intensities from a polycrystalline sample are shown as the stick spectrum (2), taken from the standard XRD data file. The patterns are normalized to the (111) diffraction.

NTs often appeared in a fused state. But they maintained their stacking property. NTs when grown to larger size by the treatment with excess Au^{3+} and ascorbic acid could even be imaged with optical microscopy (Fig. 3(B)).

In order to demonstrate the high SERS activity of the NTs, we conducted a comparative study of the SERS activity of the NTs and a monolayer assembly of Au@citrate NPs of the size >20 nm, synthesized by the Turkevich method.¹⁴ The SERS property was investigated using crystal violet molecules. We measured the SERS spectrum at various concentrations of CV adsorbed on NTs and NPs. In the typical experiment, 10 μL of CV solution of various concentrations was drop-casted on the substrate. In the case of NPs-coated substrate, a solution of 10^{-6} M CV showed a distinct SERS spectrum, which contains all the vibrations characteristics of CV molecules.

At a lower concentration, beyond 10^{-6} M, no distinct Raman signals were observed. At 10^{-7} M CV, the spectrum

was looking almost similar to that obtained from blank ITO. Figure 4(A) shows the SERS spectra taken at various concentrations of CV spotted on NPs-coated ITO. But in the case of NTs-coated substrate, it was found that even at a concentration of 10^{-10} M, the CV molecules adsorbed on NTs showed well defined Raman features (Fig. 4(B)). We repeated the same experiment using a blank conducting glass and drop-casted 10 μL of 10^{-10} M CV. There were no signals observed at 10^{-10} M of CV adsorbed on a blank ITO plate. Even at 10^{-8} M of CV, no distinct Raman signals were observed from the blank ITO. The SERS enhancement factors were calculated¹⁵ for CV molecules adsorbed on the NTs and NPs and the values were of the order of $\sim 4 \times 10^8$ and $\sim 5 \times 10^4$, respectively.

It is known that the highly localized plasmon modes could be generated at the interparticle spacing between the NPs.¹⁶ These sites are often referred to as “hot spots.”

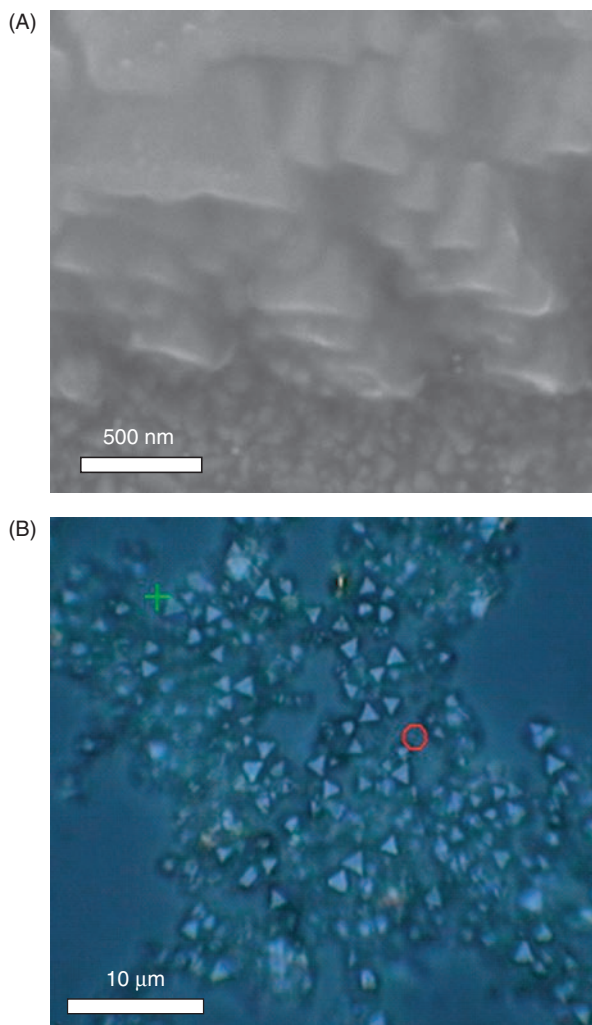


Fig. 3. (A) SEM image of the NTs formed on the ITO surface. The stacking of the NTs is clear in the image. (B) An optical image of larger uniform NTs grown on ITO.

The reason for the enhancement of the observed spectral characteristics of the CV molecule is the confinement of the molecules in these hot spots of the nanostructures. In the case of NTs, they are well stacked and each triangle is close to each other so that inter-particle spacing will be less. This creates large number of hot spots. The molecules sitting in close proximity to these sites experience an exceptionally large electromagnetic field. These large electromagnetic fields at the hot spots of the NTs act as optical traps for the CV molecules and yield enhanced scattering signals. SERS property also depends on the shape of the nanoparticles.¹⁷ The large field enhancement at the tips of each triangle also increases the SERS activity. In the case of spherical NPs, they are randomly distributed on the substrate. Since these are monolayers, the probability of two particles to come closer will be comparatively less. It is established¹⁶ that increase in the inter-particle separation distance results in decrease in the SERS intensity of the analyte molecules. Therefore, the number of hot

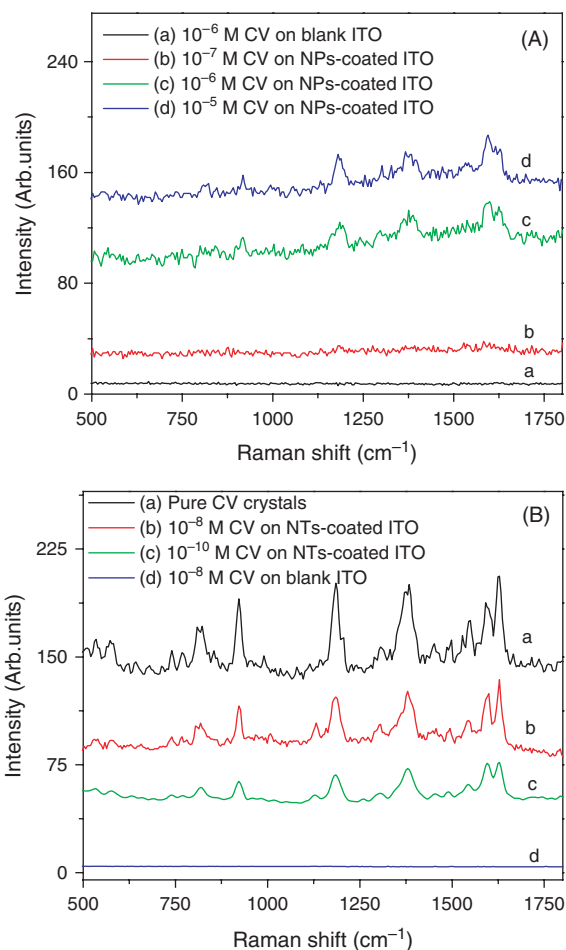


Fig. 4. The SERS spectra of CV solution of various concentrations adsorbed on (A) NPs-coated ITO and (B) NTs-coated ITO.

spots will be relatively less in the NPs assembly than in the stacked NTs.

4. CONCLUSIONS

In conclusion, we have demonstrated the high SERS activity of the uniform and oriented equilateral gold NTs synthesized on ITO surface via an electric field assisted seed-mediated approach. Shape effects of gold nanoparticles on SERS properties were investigated and found that NTs show an extremely strong SERS property than the spherical NPs. The SERS enhancement factor is calculated for both NTs and NPs, which was very high in the case of NTs. The NTs were characterized by UV-vis NIR spectroscopy, SEM, AFM and XRD. These NTs would have promising applications in surface enhancement spectroscopic methods, infrared filters and biosensors.

Acknowledgments: We thank Department of Science and Technology, Government of India for constantly supporting our research program on nanomaterials. C. Subramaniam is thanked for assistance.

References and Notes

1. (a) S. Nie and S. R. Emory, *Science* 275, 1102 (1997); (b) A. Campion and P. Kambhampati, *Chem. Soc. Rev.* 27, 241 (1998); (c) M. G. Albrecht and J. A. Creighton, *J. Am. Chem. Soc.* 99, 5215 (1977).
2. (a) X. Zhang, M. A. Young, O. Lyandres, and R. P. Van Duyne, *J. Am. Chem. Soc.* 127, 4484 (2005); (b) D. S. Grubisha, R. J. Lipert, H.-Y. Park, J. Driskell, and M. D. Porter, *Anal. Chem.* 75, 5936 (2003).
3. R. Dornhaus, M. B. Long, R. E. Benner, and R. K. Chang, *Surf. Sci.* 93, 240 (1980).
4. F. J. Adrian, *J. Chem. Phys.* 77, 5302 (1982).
5. L. Qin, S. Zou, C. Xue, A. Atkinson, G. C. Schatz, and C. A. Mirkin, *Proc. Natl. Acad. Sci.* 103, 13300 (2006).
6. S. S. Shankar, A. Rai, B. Ankamwar, A. Singh, A. Ahmad, and M. Sastry, *Nat. Mater.* 3, 482 (2004).
7. C. L. Haynes and R. P. Van Duyne, *Nano Lett.* 3, 939 (2003).
8. A. A. Umar and M. Oyama, *Cryst. Growth Des.* 6, 818 (2006); P. R. Sajanlal and T. Pradeep, *J. Chem. Sci.* 120, 79 (2008).
9. G. P. Wiederrecht and Y. Sun, *Small* 3, 1964 (2007).
10. D. Jia and A. Goonewardene, *Appl. Phys. Lett.* 88, 53105 (2006).
11. P. R. Sajanlal and T. Pradeep, *Adv. Mater.* 20, 980 (2008).
12. (a) H. Liao and J. H. Hafner, *Chem. Mater.* 17, 4636 (2005); (b) F. Kim, J. H. Song, and P. D. Yang, *J. Am. Chem. Soc.* 124, 14316 (2002).
13. J. E. Millstone, S. Park, K. L. Shuford, L. Qin, G. C. Schatz, and C. A. Mirkin, *J. Am. Chem. Soc.* 127, 5312 (2005).
14. J. Turkevich, P. L. Stevenson, and J. Hillier, *Discuss. Faraday Soc.* 11, 55 (1951).
15. G. V. Pavan Kumar, S. Shruthi, B. Vibha, B. A. A. Reddy, T. K. Kundu, and C. Narayana, *J. Phys. Chem. C* 111, 4388 (2007).
16. L. Gunnarsson, E. J. Bjerneld, H. Xu, S. Petronis, B. Kasemo, and M. Kall, *Appl. Phys. Lett.* 78, 802 (2001).
17. E. Hao and G. C. Schatz, *J. Chem. Phys.* 120, 357 (2004).

Received: 28 April 2008. Revised/Accepted: 7 August 2008.